Optimal operation planning of V2G-equipped Microgrid in the presence of EV aggregator

Published source: http://dx.doi.org/10.1016/j.epsr.2017.07.015

Optimal operation planning of V2G-equipped Microgrid in the presence of EV aggregator

B. Aluisio, A. Conserva, M. Dicorato, G. Forte, M. Trovato

Department of Electrical and Information Engineering,

Politecnico di Bari, Bari, Italy

e-mail: giuseppe.forte@poliba.it

***Abstract*:** An optimal day-ahead operation planning procedure for Microgrids (MGs) integrating Electric Vehicles (EVs) in vehicle-to-grid (V2G) configuration is described in this work. It aims to determine the day-ahead operation plan by solving a non-linear optimization procedure involving daily cost and subject to dynamic operating constraints. The day-ahead operation plan aims to minimize MG operation daily costs, according to suitable load demand and source availability forecast, in the presence of an EV aggregator. In order to account for possible economic relationships between the EV aggregator and the MG operator, two different objective functions are considered. In order to investigate the influence of EV aggregator role on MG optimal operation management in different frameworks, the proposed approach is applied to a test MG taking into account residential or commercial customers' load and EV exploitation profiles.

Keywords: Microgrid, Operation Planning, Vehicle-to-grid, Electric vehicle aggregator.

1. Introduction

The integration of large amount of distributed energy resources and of Electric Vehicles (EVs) has introduced several challenges to the planning and operation of modern electric power system [1]. The lack of coordination of Distributed Generation (DG) sources and EV charge/discharge can give rise to issues such as reverse flows, unintentional islanding, overloads. To cope with these concerns, Microgrids (MGs) able to integrate DG technologies, Energy Storage Systems (ESSs) and charging station, as well as electric and thermal loads, are more and more employed [2][3]. The recent diffusion of EVs in Vehicle-to-Grid (V2G) configuration, along with station technological improvement, has also shifted EV role from heavy loads to small-sized distributed virtual generator. V2G scheme can be adopted for providing regulation services to the distribution grid, as illustrated in [4]-[9], whereas the influence of V2G system on MG operation is evaluated in [10]-[13].

The EV charging process (or energy exchange in V2G configuration) can be optimally managed in order to provide economic benefit to EV owners and to support MG operation, particularly when a fleet constituted by several EVs is plugged into the grid simultaneously at the same connection point [14]. In this case, the MG operator interacts with vehicle fleets through EV aggregators, which provide appropriate control of the parked vehicles and their interaction with the grid [15]. The EV aggregator is in charge of performing the “smart charging” service, by exploiting time flexibility given by the difference between needed charging time and parking time to provide grid services and meet the needs of the driver [16]. The EV aggregator performs the smart charging service by determining how and when each vehicle is to be charged, thereby providing a demand-dispatch service to a utility or grid operator [17].

One of the main goals of MG operator is to elaborate a suitable operation plan in the day-ahead horizon, in order to program its units accounting for economic burdens, environmental impact and reliability issues [18][19][20]. For the development of procedures for MG day-ahead operation planning, different approaches are present in literature to take into account the variability of PV and wind production, load demand, energy prices, EV parking intervals

Published source: http://dx.doi.org/10.1016/j.epsr.2017.07.015

and energy requirements. A distinction can be made among stochastic methods accounting for possible deviations of forecasts with proper probability distribution functions (pdfs) [21]-[23], procedures based on the generation of different scenarios with relevant probability [24]-[28], and methodologies based on deterministic data [33]-[39]. The proposed approach falls in this last field, i.e. considering as inputs the most probable value of the forecasts of different quantities subject to prediction instead of decision, since it represents the most realistic form to determine plans to be implemented by actual SCADA in MGs. For this reason, advanced prediction methods should be accounted [40][41][42], that are beyond the scope of the paper. Moreover, even exploiting stochastic methods (e.g. chance constrained, robust optimization, …), the presence of variation during operation outside the pdfs or not considered in scenarios will cause a different behaviour with respect to the plan. It should be observed that the risk reduction due to stochastic optimization is not remarkable in this case with respect to a deterministic procedure with suitable operation margins of the devices [36]. Therefore a second-stage procedure, closer to real time operation and entrusted to cope with those variations, operating over shorter time intervals (e.g. an hour or a group of hours) and accounting for even faster variations (down to minutes or some seconds), should be carried out as indicated also in [11], [29]-[32], [33], [35], [38], [43].

In this paper, a procedure for MG operation planning able to integrate EV fleet management is carried out adopting a non-linear daily cost minimization subject to dynamic operating constraints. With respect to analogous multiobjective approaches, based on suitably forecasted generation of renewable-based sources and load demand [44]-[47], the proposed optimization procedure further allows to assess benefits from EV fleet in V2G configuration, by accounting the EV aggregator role. In particular, it is envisaged that MG operator and EV aggregator could be either separate entities or represent a unique entity, implying different objectives for MG operator during the elaboration of the optimal plan. The methodology is applied to a test MG including several devices for electric and thermal power production and storage, along with V2G systems, in charge to satisfy energy needs at premises of residential or commercial users, where the presence of EVs is creating new opportunities for the implementation of MG [48][49] and the constitution of EV aggregator can be conceived.

The following novelty issues of this work can be pointed out:

- The influence of V2G technology for EV fleet in the frame of MG for thermal and electric energy supply;
- The adoption of realistic models for energy storage devices and combined heat and power systems;
- The analysis of different interactions between EV aggregator and MG operator on techno-economic basis;
- A particular care on EV use patterns according to the different users.

The remainder of the paper is organized as follows. In Section 2, a formalization of device models and of MG operation planning problem is included. Section 3 is devoted to the explanation of test system and to the illustration and discussion of simulation results. Concluding remarks are discussed in Section 4.

2. MG Operation Planning

2.1. Modeling of MG devices

The setup of a proper formulation starts from modelling of the involved energy equipment. Different kinds of devices can be individuated: fuel-based energy production systems (caring for electricity or thermal energy, or even both in cogeneration layout), renewable-based generation devices, energy storage systems, grid connection, EVs, energy consumption. In order to represent the time variation of energy flows, the daily horizon is divided in N_t time steps with a time width of Δt each, typically ranging between 5 minutes to 1 hour [50],

Published source: http://dx.doi.org/10.1016/j.epsr.2017.07.015

compatibly with granularity of day-ahead forecast methods ensuring acceptable uncertainty levels [40][41][42]. Since MG-sized devices react to power reference variations reaching the required condition in some seconds [51][52], the adoption of static models allows a powerful representation of the devices in the described time steps without losing accuracy.

In particular, the *i*-th fuel-based production device can work at any electric production level $P(i,t)$, within its technical features, although fuel procurement is incurred and local emissions are produced. Therefore, its operation can be characterized by determining fuel consumption $F(i,t)$ and emission amount $E(i,t)$ and bounding production level through the following relations:

$$F(i,t) = \frac{\Delta t \cdot P(i,t)}{fv(i) \cdot \eta_E\left(P(i,t)\right)} \tag{1.a}$$

$$E(i,t) = \varepsilon\left(P(i,t)\right) \cdot \Delta t \cdot P(i,t) \tag{1.b}$$

$$P^m(i) \leq P(i,t) \leq P^M(i) \tag{1.c}$$

where $fv(i)$ represents fuel heating value, and electric efficiency $\eta_E\left(P(i,t)\right)$ depends on power production level through a polynomial function. Since emissions are related to fuel energy consumption, emission factor $\varepsilon\left(P(i,t)\right)$ is inversely proportional to electric efficiency, i.e. $\varepsilon\left(P(i,t)\right) = k\varepsilon(i) / \eta_E\left(P(i,t)\right)$, where $k\varepsilon(i)$ is a constant factor depending of the technology of the *i*-th fuel-based production device. Moreover $P^m(i)$ and $P^M(i)$ stand for minimum and maximum power output, respectively. The use of discrete variables for on-off status of generators accounting for experimental nonlinear efficiency functions would involve MINLP formulation, although it could not lead to feasible results [53] and does not involve remarkable advantage with respect to NLP. Therefore, the proposed NLP formulation allows to ensure convergence and to lose as low information as possible.

In the case of simple thermal energy production, the previous formulations keep valid by expressing the quantities in terms of heat production level $Q(i,t)$:

$$F(i,t) = \frac{\Delta t \cdot Q(i,t)}{fv(i) \cdot \eta_T(Q(i,t))} \tag{2.a}$$

$$E(i,t) = \varepsilon_T(Q(i,t)) \cdot \Delta t \cdot Q(i,t) \tag{2.b}$$

$$Q^m(i) \le Q(i,t) \le Q^M(i) \tag{2.c}$$

where thermal efficiency, $\eta_T(Q(i,t))$, unitary emission factor per thermal energy $\varepsilon_T(Q(i,t))$ (inversely proportional to thermal efficiency) and minimum and maximum thermal power, $Q^m(i)$ and $Q^M(i)$ are considered.

For the representation of MG-sized cogeneration systems, a direct correlation between electric power production $P(i,t)$ and heat production $Q(i,t)$ is adopted, as suggested in [43][54][55], that proves more appropriate than other possible representations, such as feasible electricity-heat operating region reported in [56]. Therefore, either electric or thermal power represent the decision variable, since the following relation holds:

$$Q(i,t) = \frac{\eta_T(Q(i,t))}{\eta_E(P(i,t))} \cdot P(i,t) \tag{3}$$

As regards the *r*-th technology based on a non-programmable renewable energy source (RES), e.g. wind, solar radiation, water flow, relevant power production level $P(r,t)$ or thermal production level $Q(r,t)$ can be obtained by forecasting source availability, and accounting for the specific function of energy conversion, e.g. wind turbine power related to speed and PV panel conversion according to solar radiation and temperature effects [57].

Energy storage devices are characterized by internal state of charge $S(s,t)$. For the *s*-th storage system, this quantity is related to electric power charge/discharge of the device

Published source: http://dx.doi.org/10.1016/j.epsr.2017.07.015

($P_c(s,t)$ and $P_d(s,t)$, respectively) and to technical features of the system through the following expressions:

$$S(s,t)=S(s,t-1)+\psi_c(s)\cdot\Delta t\cdot P_c(s,t)-\frac{P_d(s,t)}{\psi_d(s)}\cdot\Delta t-\rho(s)\cdot S^M(s) \tag{4.a}$$

$$S^m(s)\le S(s,t)\le S^M(s) \tag{4.b}$$

$$0\le P_c(s,t)\le P_c^M(s) \tag{4.c}$$

$$0\le P_d(s,t)\le P_d^M(s) \tag{4.d}$$

$$P_c(s,t)\cdot P_d(s,t)=0 \tag{4.e}$$

$$S(s,0)-\psi_c(s)\cdot\Delta t\cdot P_c^M(s)\le S(s,N_t)\le S(s,0)+\frac{P_d^M(s)}{\psi_d(s)}\cdot\Delta t \tag{4.f}$$

In (4.a), $S(s,t-1)$ is the state of charge at previous time step. The initial state of charge of the considered day $S(s,0)$ corresponds to the final state of charge at the end of the previous day, that is a known value for the operation planning of the considered day. Moreover, $\psi_c(s)$ and $\psi_d(s)$ are charge and discharge efficiency, respectively, $S^M(s)$ and $S^m(s)$ are the maximum and minimum charge capacity, respectively, $P_c^M(s)$ and $P_d^M(s)$ are the maximum charge and discharge rates, respectively, and $\rho(s)$ is the self-discharge rate. Equation (4.e) avoids charge and discharge of the device in the same period. Constraint (4.f) bounds the final state of charge of the considered day in an narrow range around the initial state of charge of the considered day. This assumptions ensures more flexibility to the use of ESS and allows to account for self-discharge. In other works as [20][39][58] initial and final values in the considered day are equal, whereas in [59][60] this range is considered as a defined percentage of maximum charge capacity. In the proposed constraint (4.f), range limits correspond to maximum variation of the state of charge that the ESS can perform in a single time step. ESS parameters depend on the lifetime of the device due to degradation phenomena, however, for the investigation of a single day, they are univocally determined referring to the specific ESS lifetime condition.

Electric connection to the distribution grid is characterized by amounts of power purchase $P_{Pur}(t)$ and power injection $P_{Inj}(t)$. Since the connection is usually only one for a MG, power exchange can occur in only one direction per each time step. Including technical limits, the following relations hold:

$$0 \le P_{Pur}(t) \le P_{Pur}^{M}(t) \tag{5.a}$$

$$0 \le P_{Inj}(t) \le P_{Inj}^{M}(t) \tag{5.b}$$

$$P_{Pur}(t) \cdot P_{Inj}(t) = 0 \tag{5.c}$$

where $P_{Pur}^{M}(t)$ and $P_{Inj}^{M}(t)$ are the maximum electric power purchasable and deliverable at grid connection, respectively.

The behavior of an EV fleet in V2G configuration, managed by an aggregator, can be modelled analogously to an ESS, although the EV fleet is connected to the grid only in selected time periods. Let *j* be the interval (set of time steps) for which the *v*-th EV fleet is parked, and therefore for that *j*-th interval, define $t_A(v,j)$ as the forecasted time step when the *v*-th EV fleet arrives to the station with energy content $S(v,t_A(v,j))$, and $t_L(v,j)$ as the forecasted time step at which the *v*-th EV fleet leaves the station with energy content $S(v,t_L(v,j))$. Hence, the following relations are valid for each time step of the *j*-th stationing interval, considering that the energy exchange process can start a time step after the arrival [24], i.e. $t_A(v,j)+1 \le t \le t_L(v,j)$.

$$S(v,t) = S(v,t-1) + \psi_c(v) \cdot \Delta t \cdot P_c(v,t) - \Delta t \cdot \frac{P_d(v,t)}{\psi_d(v)} \tag{6.a}$$

Published source: http://dx.doi.org/10.1016/j.epsr.2017.07.015

$$S^m(v) \le S(v,t) \le S^M(v) \tag{6.b}$$

$$0 \le P_c(v,t) \le P_c^M(v) \tag{6.c}$$

$$0 \le P_d(v,t) \le P_d^M(v) \tag{6.d}$$

$$P_c(v,t) \cdot P_d(v,t) = 0 \tag{6.e}$$

All the terms assume the same meaning with respect to (4.a)-(4.e), but referred to the *v*-th EV fleet instead of the *s*-th energy storage. Self-discharging effect can be neglected for the EVs [61]. The presence of several parking intervals of the same EV fleet during the day can be considered. In particular, the case of a night parking of the EV fleet is dealt with by assuming at least two intervals, one starting at the first time step of the day and one ending at the last time step of the day. In order to account for a continuity of EV charging, it is assumed that the energy state of EV fleet at the extreme time steps in the day, pertaining to different parking intervals, is the same, i.e. $S(v,1) = S(v,N_t)$. Moreover, the maximum power amount in charge and discharge phase ($P_c^M(v)$ and $P_d^M(v)$, respectively) are affected by technical features of the EVs, of the charging/V2G stations and of the connection network.

The energy demand of final users in the MG is represented by electricity loads $P_L(k,t)$ and thermal loads $Q_L(h,t)$. It is assumed that in MG context all the loads are connected to the same electric distribution system, that is mainly realized in MG context by means of radial schemes covering at most distances of few hundred meters. In this framework, if the network is well-designed, voltage magnitudes are close to nominal value and angle displacements are small, therefore no power flow violations are expectable and power losses can be negligible [20][21][25]. Analogously, all thermal loads are considered to refer to a well-designed heat distribution system with negligible losses. Therefore, the satisfaction of the internal demand can be represented by means of copperplate balance relations, as follows:

$$\begin{aligned}&\sum_{k=1}^{N_L} P_L(k,t)+\sum_{s=1}^{N_S} P_c(s,t)+\sum_{v=1}^{N_V} P_c(v,t)+P_{Inj}(t)=\\&=\sum_{i=1}^{N_G} P(i,t)+\sum_{r=1}^{N_R} P(r,t)+\sum_{s=1}^{N_S} P_d(s,t)+\sum_{v=1}^{N_V} P_d(v,t)+P_{Pur}(t)\end{aligned} \tag{7}$$

$$\sum_{j=1}^{N_H} Q_L(h,t)\le \sum_{i=1}^{N_G} Q(i,t)+\sum_{r=1}^{N_R} Q(r,t) \tag{8}$$

In (7), N_L represents the total number of electric loads, N_S is the number of energy storage systems, N_V represents the number of EV fleets, whereas in (8) N_H is the number of thermal loads. In both equations, N_G stands for the number of fuel-based generation facilities, and N_R represents the number of RES-based energy production devices.

It should be remarked that the electric power balance is expressed by an equality, since the electricity cannot be wasted, whereas thermal balance is expressed by an inequality, allowing the flexibility to release excess heat in the atmosphere (useful for CHPs) or leaving room to thermal energy storage devices, that are beyond the scope of this work.

2.2. Problem formulation and objective functions

The goal of the operation planning is to minimize an objective function according to feasibility constraints, as per the following expression:

$$\begin{aligned}&\min f(\mathbf{x})\\&\text{s.t.}\begin{cases} g(\mathbf{x})=0\\ h(\mathbf{x})\le 0\end{cases}\end{aligned} \tag{9}$$

The state variable vector **x** includes power production/exchange profiles for the controllable sources (fuel-based generators, energy storage, EV fleets, grid connection) over the daily horizon, along with the state of charge of energy storage devices and EVs. The set of equality constraints $g(\mathbf{x})=0$ includes (3), (4.a), (4.e), (5.c), (6.a), (6.e) and (7), whereas inequality constraints $h(\mathbf{x})\le 0$ include (1.c), (2.c), (4.b)-(4.d), (4.f), (5.a)-(5.b), (6.b)-(6.d) and (8).

Several objectives can be posed to MG operation planning, optimizing economic, environmental and technical aspects [61]. In this paper, a hybrid objective function is accounted, including total variable costs for MG operation and properly weighed equivalent CO_2 emission cost, to provide for feasible production programs with limited environmental impact.

The objective function can be expressed as the sum of different terms related to the devices described in the previous section. In particular, actualized investment cost is neglected, along with variable costs for RES-based technologies, since maintenance is quite inexpensive [62], and for ESSs, as the effort for keeping the system in correct operation is already taken into account by the self-discharge amount.

The role of EV aggregator is to manage the process of energy exchange of EVs. It is assumed that the EV stations are physically connected to the MG and not directly linked to the distribution network. Variable cost related to EV management depends on the relationship between EV aggregator and MG operator, as described in Fig. 1.

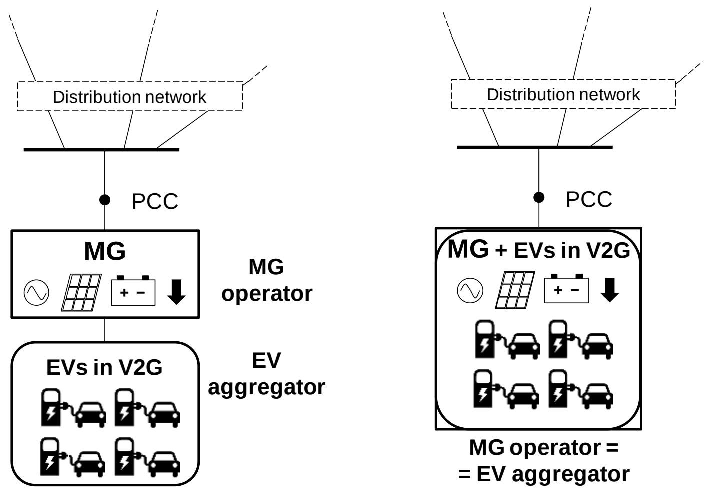

Fig. 1. Different relations between MG operator and EV aggregator

In the first case, the EV aggregator is a distinct entity that has concluded a specific contract for the electricity exchange in each direction with the MG operator. The MG operator is in charge of exchanging power with the distributor (see left side of Fig. 1). This condition can

Published source: http://dx.doi.org/10.1016/j.epsr.2017.07.015

reproduce the presence of an EV management entity at residential premises or for EV parking lot adjacent to a commercial or tertiary activity. Under these assumptions, the objective function of MG operator in the first case $f_1(\mathbf{x})$ can be defined as follows:

$$f_1(\mathbf{x}) = \sum_{t=1}^{N_t} \Delta t \cdot \Bigg\{ \left[\pi(t) P_{Pur}(t) + \sum_{i=1}^{N_G} \varphi(i) F(i,t) \right] + \sigma \left[\varepsilon_P P_{Pur}(t) + \sum_{i=1}^{N_G} E(i,t) \right] - \beta(t) P_{Inj}(t) + \sum_{v=1}^{N_V} \left[\xi(t) P_c(v,t) - \chi(t) P_d(v,t) \right] \Bigg\} \quad (10)$$

where $\pi(t)$ and $\beta(t)$ represent electricity purchase cost and electricity delivery price, respectively, in the t-th time step. Moreover, $\xi(t)$ and $\chi(t)$ are the electricity purchase cost for EV charging and the electricity delivery price for V2G discharging, respectively. Finally, $\varphi(i)$ is the fuel price for the i-th fuel-based generator, σ is the penalty cost applied to the CO_2 emissions and ε_P is the average emission factor related to electricity coming from the external grid.

In the second case, the role of EV aggregator is in charge to the MG operator. With this outline, the EV fleet is considered and managed as a MG energy source. Therefore, one of the major interests of the unique managing subject would be to preserve lifetime of EVs avoiding deep cycling operation, along with supplying energy to the MG and to EVs for covering travel needs, at reasonable cost (see right side of Fig. 1). This scheme can be realized by the energy management body of a residential complex detaining EVs as well, or in the presence of service vehicles owned by a factory or a public body. The objective function of MG operator in this second case $f_2(\mathbf{x})$ can be written as:

$$f_2(\mathbf{x}) = \sum_{t=1}^{N_t} \Delta t \cdot \Bigg\{ \left[\pi(t) P_{Pur}(t) + \sum_{i=1}^{N_G} \varphi(i) F(i,t) \right] + \sigma \left[\varepsilon_P P_{Pur}(t) + \sum_{i=1}^{N_G} E(i,t) \right] - \beta(t) P_{Inj}(t) + \sum_{v=1}^{N_V} \omega(v) P_c(v,t) \Bigg\} \quad (11)$$

where $\omega(v)$ is the wearing cost of the v-th EV fleet, taking into account the actualization of EV battery cost over the forecasted throughput during the provided battery lifetime [36][63][64], obtained as the product of nominal capacity by the provided number of cycles at the target depth of discharge $S^M(v)-S^m(v)$ [65], Therefore, the wearing cost is determined *a priori*, as an input of the problem, once the technology of EV battery and the desired depth of discharge are defined, and it is applied to the equivalent cycle given by charge power $P_c(v,t)$.

It should be remarked that both $f_1(\mathbf{x})$ and $f_2(\mathbf{x})$ represent the total daily cost of MG operator with different economic treatment of EV energy. In $f_1(\mathbf{x})$, the exchange of energy between MG operator and EV aggregator is ruled by a contract with different rates for EV charge and discharge. In $f_2(\mathbf{x})$, EVs are dealt with just as other internal MG sources, and MG operator aims to minimize the production costs, that for EVs are represented by wearing costs. Each function is therefore minimized in the presence of the same inputs, and relevant results are compared in order to investigate the effectiveness of different relations between MG operator and EV aggregator. Having MG a size of some hundreds of kW, MG operator is not called to actively participate in market sessions and to deal with relevant risk, but it acts as a price taker, in accordance with various analogous approaches [22][58][67]. According to this assumption, $\pi(t)$ and $\beta(t)$ account for a proper forecast of market prices and for additional burdens according to specified tariff schemes.

3. Case Study and Results

3.1. Test system characterization

In order to investigate the performance of the proposed procedure along with its possible application, a case study is carried out, based on a test MG reproducing the features of an experimental facility realized at the Power and Energy System Laboratory of Politecnico di Bari [66] with provisional enhancements. Site-dependent data, i.e. renewable source availability and meteorological data affecting energy demands and yields, are referred to forecasts derived from historical data at the laboratory location.

The MG includes as generation sources a gas-based Internal Combustion Engine (ICE) in cogeneration mode, a Microturbine (MT) in cogeneration mode, a PV plant, a wind emulator to replicate various wind turbine (WT) response to wind speed. Moreover, an energy storage system and a fast-charging V2G station are provided, and programmable loads can simulate the presence of different consumers as well. A boiler section is considered in order to underpin the thermal demand coverage. The features of the components are reported in the following Tables 1, 2 and 3 for RES devices, energy production and energy storage, respectively, along with the relevant name exploited in the test. The parameters are derived from nameplate data of the devices included in the experimental facility, or obtained by relevant characterization tests, or taken from literature references where indicated. The case study includes a daily horizon subdivided in 96 time steps with a duration of 15 minutes. For CHP1 and CHP2, trends of electric efficiency are reported in Fig. 2. Thermal efficiencies for CHPs and Boilers are considered constant, since no remarkable variation is observed. Therefore, as can be derived from comments to (1.b) and (2.b), emission factor is inversely proportional to electric efficiency for CHPs, whereas for boilers it is constant at rated value. Moreover, minimum production level for CHPs is set to zero, compatibly with observed low minimum stable production (roughly 1 kW).

Table 1. Test MG – Renewable Based Generator Features

Device name	Device type	Rated electric power [kW]
PV 1	Mono-crystalline silicon	20
PV 2	Poly-crystalline silicon	20
PV 3	Amorphous thin film PV	20
WT 1	Horizontal axis WT	40
WT 2	Vertical axis WT	20

Published source: http://dx.doi.org/10.1016/j.epsr.2017.07.015

Table 2. Test MG – Energy Production Devices Features

Device name	Device type	Rated electric/thermal power [kW]	Rated electric/thermal efficiency [%]	Rated emission factor [kg/kWh]
CHP 1	ICE	105 / 185	31.5 / 56	0.594
CHP 2	MT	28 / 57	25 / 50	0.725
HB 1	Wood boiler	--- / 75	--- / 82.5	0.02
HB 2	Pellet boiler	--- / 20	--- / 88.2	0.00
Grid	Power exchange	80 / ---	---	0.309 [68]

Table 3. Test MG – Energy Storage device features

Device name	Device type	Rated capacity [kWh]	Rated electric power [kW]	Charge/ discharge efficiency [%]	Self-discharge rate [%/h]
ESS	Na-Ni battery	180	48	85	1.36
EVs	10-EV fleet with 10 V2G stations	240	100	90.9 [69]	---

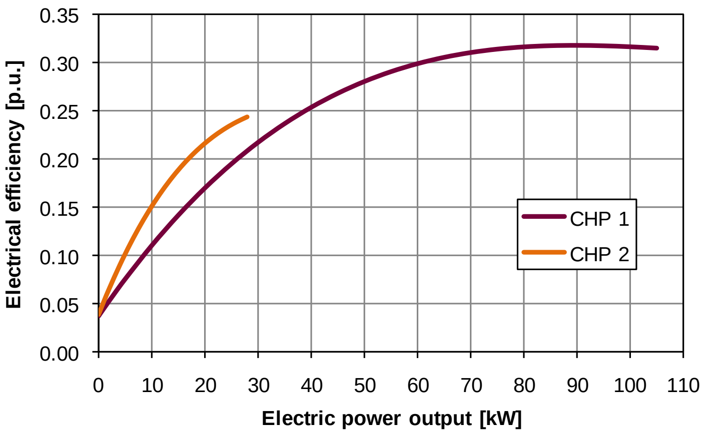

Fig. 2. Electrical efficiency curve of the CHPs.

The case study considers a typical winter day with residential and commercial load supplied by the MG. Power and heat demand curves for users are taken from U.S. data in [70] and accounting for similar climate conditions with respect to the location of the experimental facility. User features are reported in Table 4.

In the considered day, the total forecasted RES production is equal to 334.4 kWh, covering 14.7% of the residential load and 19.3% of the commercial one. It is worth to remark that wind contribution is higher than PV yield.

Table 4. Test MG – User features

User Description	Electric / thermal peak power [kW]	Electric / thermal daily demand [kWh]
Residential 50 twin apartments	160 / 250	2,278.5 / 3,911.5
Commercial Medium-size office	140 / 250	1,731.5 / 2,167.3

In order to best exploit the potential of MG components and not to jeopardize the security of system in emergency cases, as involuntary islanding, the allowed exchange of electric power with the distribution network is limited at 80 kW.

In the EV parking lot 10 V2G charging stations are installed. In Figure 2 the EV fleet connection to the V2G charging station is characterized by time intervals depending on dwellers and employees behaviour for residential and commercial building, respectively. In particular, in the residential case (upper part of Fig. 3), parking interval starts at 6:45 p.m. at 60% charge (red) and ends at 8 a.m. at 80% (green), therefore two intervals are included in simulation, as described in Section II, involving the continuity of energy content variation at extremes of the day (blue). Whereas, for the office building (lower part of Fig. 3), clerks arrive at workplace at 8 a.m. with 40% charge (red) and leave at 6:30 p.m. at 80% (green), with a single parking interval.

The energy content of the EVs at station leaving is supposed at 80% of rated capacity, to decrease the effects of range anxiety [71] as well as to ensure the presence of suitable margins for V2G exploitation and for successive adjustments in the framework of second-stage procedure for real time management. The state of charge at fleet arrival is accounted according to average routes of the EV drivers. The choice of the variation range of state of charge between 20% and 90% helps extending EVs lifetime preventing full charge and deep discharge [34][72][73]. It has to be pointed out that the link of EV exploitation of the two users is beyond the scope of the paper.

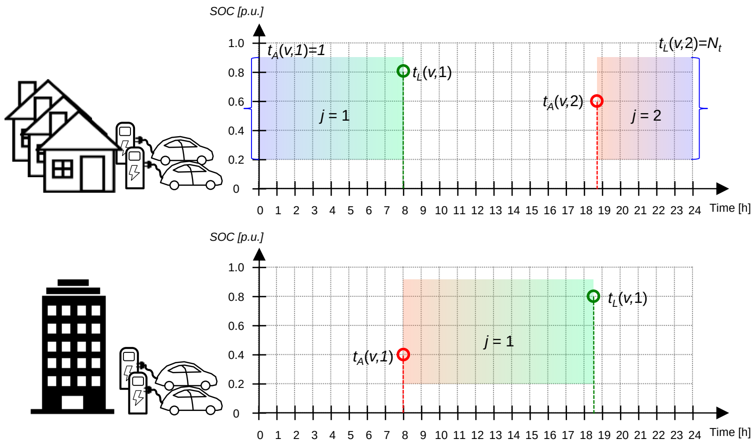

Fig. 3. EV fleet characterization for the considered users.

The electricity purchase price $\pi(t)$ is determined as sum of hourly spot market prices and additional burdens to cover transport and distribution service included in tariffs for domestic and non-domestic users, whereas electricity delivery cost $\beta(t)$ is characterized by three levels for peak, average and off-peak hours respectively, according to Italian energy service operator [74]. Fuel cost $\varphi(i)$ derives from tariffs of an Italian fuel distribution company [75] and are equal to 0.51 €/Sm^3 for gas, 0.172 €/kg for wood, 0.32 €/kg for pellet, supposed constant over the whole day. Moreover, emission cost σ is equal to 0.57 c€/kg [76].

The two formulations of the objective function of the day-ahead scheduling problem, as defined in the previous section, are both applied to the two user profiles. In particular, while considering $f_1(\mathbf{x})$, different tariff schemes are analysed, and the best solution is obtained with a flat EV discharge cost $\chi(t)$ equal to 18 c€/kW and with an EV charge price $\xi(t)$ having two levels for residential user and a constant value for the commercial one. Cost trends are reported in Fig. 4, indicating with subscribed *res* and *com* the costs for residential commercial users, respectively. When $f_2(\mathbf{x})$ is minimized, EV wearing cost $\omega(v)$ is equal to 5 c€/kWh, as in [77].

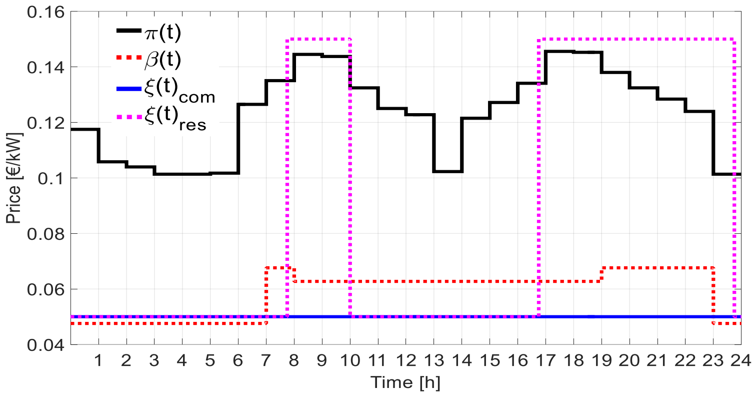

Fig. 4. Cost diagram for each time step.

3.2. Solution procedure

The optimization is performed in MatLAB® environment, exploiting *fmincon* function by means of the SQP algorithm [78]. It is a Newton-type method, characterized by super-linear convergence, and proved robust for the solution of nonlinear optimization problems, even in non-convex formulations [79][80]. Details of SQP method are reported in the Appendix.

The relative tolerance levels on decision variables, constraints and objective function are all set to $1 \cdot 10^{-4}$.

As most of the methods for nonlinear problem solution, the algorithm efficiently searches for a local minimum, therefore a proper initial condition is provided [81]. This is done through the solution of the linearized formulation of problem (9), by accounting for rated efficiencies of fuel-based devices (see Table 2) in (1.a), (1.b), (2.a), (2.b) and (3), and discarding non-contemporaneity constraints for bidirectional power exchanges (4.e), (5.c), (6.e). These constraints are verified *a posteriori*, and where they are not satisfied, the solution is corrected by subtracting to both values the minimum one. The proposed procedure to solve the non-linear problem (9) is managed automatically in all its parts, as explicated in the flowchart reported in Fig. 5, where the stages of initial solution determination (through the linearized problem) and of solution of complete NLP problem (9) are illustrated.

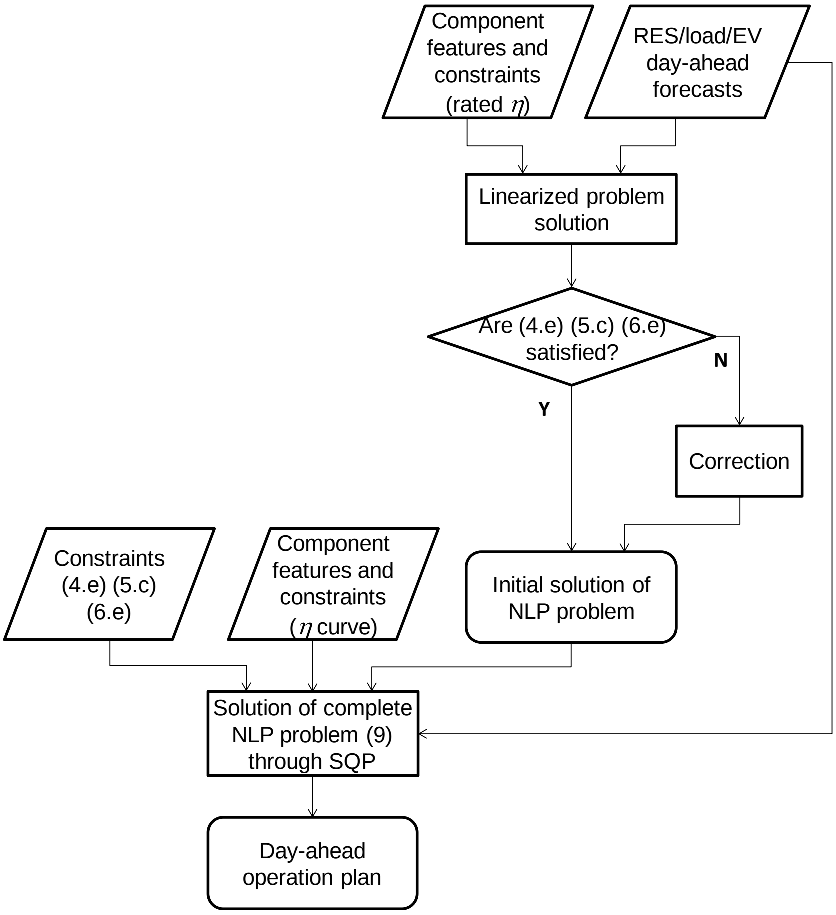

Fig. 5. Solution flowchart of the proposed day-ahead procedure.

3.3. Test cases and discussion

The results of optimal operation planning of the test MG in the presence of the described residential load are presented.

In particular, the application of the objective function $f_1(\mathbf{x})$, defined in (10), yields the results reported in Figs 6.a, 7.a and 8.a, where electric balance, thermal balance and SOC of storage devices are shown, respectively. In Fig. 8.a, positive values of power by ESS and EVs correspond to discharge power, whereas negative values stand for charge power. As regards grid power, positive values represent power purchase and negative ones correspond to delivery. It can be seen that the EV discharge guarantees the coverage of the electric load in periods when production by RES is low, for instance between hours 19 and 22, as remarked

Published source: http://dx.doi.org/10.1016/j.epsr.2017.07.015

by the SOC trend of EVs in Fig. 8.a. Moreover, the excess power production by CHPs with respect to the original load trend, along with grid withdrawal, is addressed at charging ESS and EVs. In particular, ESS is charged in central hours of the day, in the presence of remarkable RES production. EVs are charged in late evening and early morning, when electricity purchase price is lower and thermal demand drives CHP extra production. Due to low delivery price, no power injection to the main network is observed.

Whereas, the application to residential user of $f_2(\mathbf{x})$ objective, defined in (11), leads to results depicted in Figs 6.b, 7.b and 8.b. In this case, the EV SOC experiences less fluctuations, keeping constant for most of the parking interval. This is ascribable to the presence of the wearing cost, that prevents V2G to occur. EV charge is observed only in early morning, when thermal load trend involves an excess of electricity production by CHP1 with respect to the demand. The ESS is more deeply employed in the presence of EV wearing cost due to lack of EV discharge.

As regards thermal energy, the demand is covered mostly by CHP1 in both cases (see Fig. 7.a and 7.b), respecting the technical limits, whereas the CHP2 and HBs are exploited during peak demand periods.

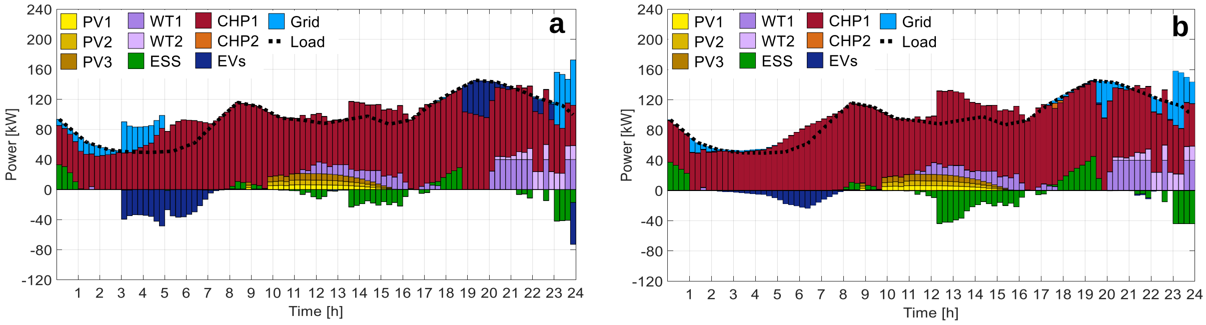

Fig. 6. Electric power balance of Residential user with $f_1(\mathbf{x})$ objective (a) and $f_2(\mathbf{x})$ objective (b).

Published source: http://dx.doi.org/10.1016/j.epsr.2017.07.015

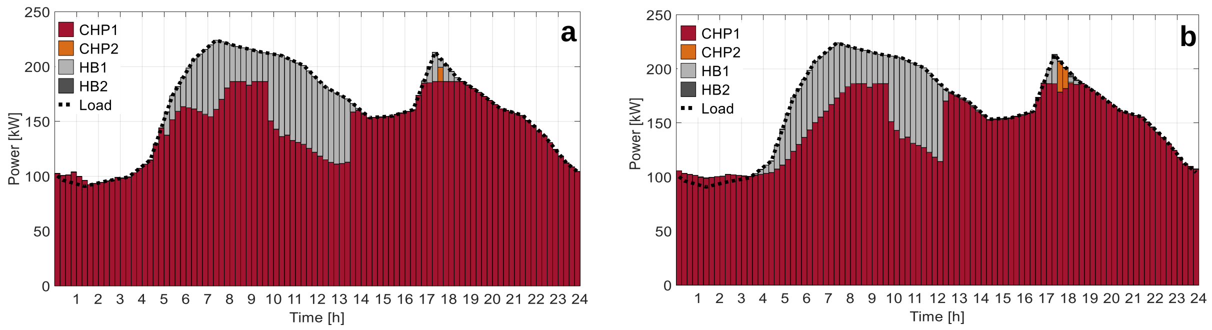

Fig. 7. Thermal power balance of Residential user with $f_1(\mathbf{x})$ objective (a) and $f_2(\mathbf{x})$ objective (b).

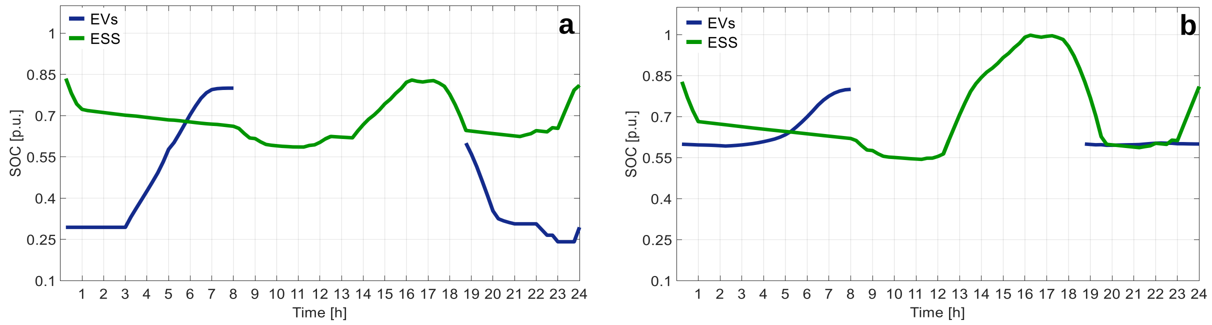

Fig. 8. Storage state-of-charge of Residential user with $f_1(\mathbf{x})$ objective (a) and $f_2(\mathbf{x})$ objective (b).

The optimal MG operation plan in the presence of commercial load is illustrated in Figs. 9.a, 10.a and 11.a in the case of $f_1(\mathbf{x})$ objective, and in Figs. 9.b, 10.b and 11.b in the case of $f_2(\mathbf{x})$ minimization. It can be noted that the different load profiles of this user involve a different exploitation of internal sources. In particular, in the first and last hours of the day, when heat is not needed, the CHPs are not fired on, since it reveals more convenient to purchase energy from the grid at low price levels rather than exploiting CHP at partial load, with low efficiency. The pursuit of $f_1(\mathbf{x})$ objective implies a deeper EV employment due to the difference of price levels. In particular, EVs are intensively charged at arrival, in central hours of the day and at the end of parking time, even withdrawing additional electricity from the grid. This trend is supported by the ESS as well, in fact ESS discharges in periods when EVs require to charge and vice versa, as shown in Fig. 11.a. However, the described curves entail a peak of total demand up to 210 kW, almost doubling the predicted load. As regards

Published source: http://dx.doi.org/10.1016/j.epsr.2017.07.015

thermal load (Fig. 10.a), according to economic and environmental merit order, the baseload is covered by the CHP1, and HBs and CHP2 are called to produce in peak periods. When the demand is low, CHP1 is less convenient than HB1.

When $f_2(\mathbf{x})$ is minimized, EVs charge only in central hours of the day, as reported in Fig. 9.b. Indeed, the saddle in thermal demand (Fig. 10.b) does not allow for intense CHP exploitation, therefore further grid withdrawal is necessary for EV charging in low-price periods. This involves a deeper discharge of ESS during hours 8-11 to cover the demand in peak price period. In all cases, self-discharge effect of ESS in idle state is observed.

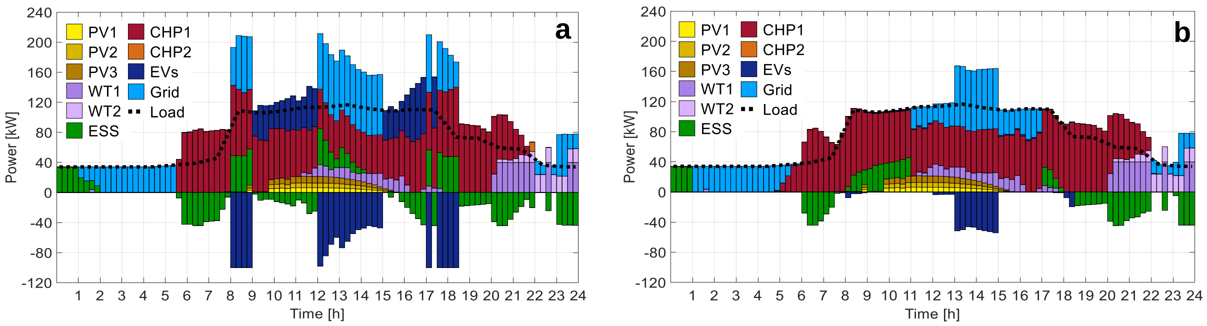

Fig. 9. Electric power balance of Commercial user with $f_1(\mathbf{x})$ objective (a) and $f_2(\mathbf{x})$ objective (b).

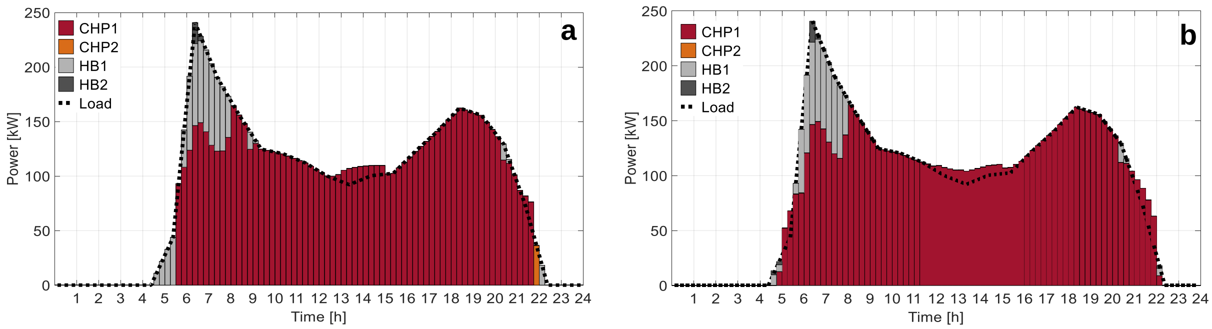

Fig. 10. Thermal power balance of Commercial user with $f_1(\mathbf{x})$ objective (a) and $f_2(\mathbf{x})$ objective (b).

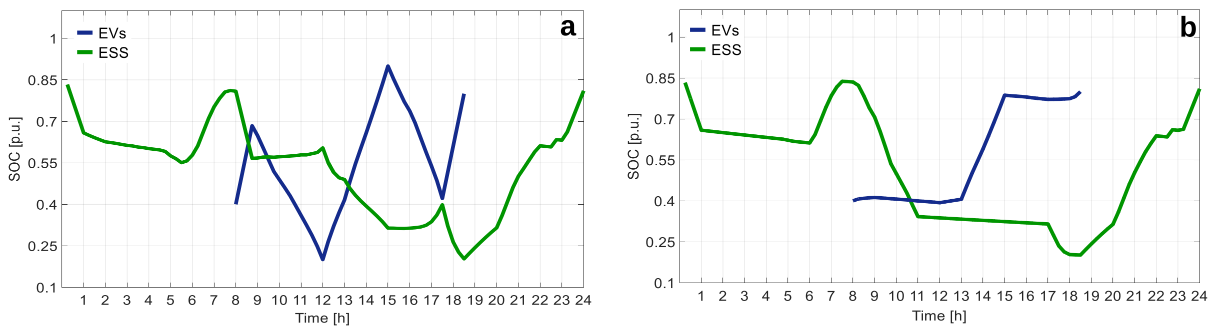

Fig. 11. Storage state-of-charge of Commercial user with $f_1(\mathbf{x})$ objective (a) and $f_2(\mathbf{x})$ objective (b).

It can be seen that the adoption of realistic electric efficiency curve, that has remarkably low values at low production levels, avoids operation of CHPs below the minimum stable generation level in all cases. In this way, analogous results are obtained with respect to other approaches introducing integer on/off variables.

The comparison of total daily costs and relevant main contributions is reported in Table 5. It allows to state that the $f_1(\mathbf{x})$ objective reveals cheaper than the $f_2(\mathbf{x})$ for both users (3% in residential case and 7% in commercial case), revealing that an *ad hoc* tariff scheme applied by the aggregator for EV charge and discharge can encourage their use for MG optimal operation purposes. Grid purchase has a higher impact for the commercial user (18-24% with respect to 3-4% for the residential one), due to the different demand trend, whereas emission costs do not affect significantly the total expenses, contributing in each case to less than 2%.

Table 5. Test MG – Daily Cost contributions [€]

	Residential		**Commercial**	
	$f_1(\mathbf{x})$	$f_2(\mathbf{x})$	$f_1(\mathbf{x})$	$f_2(\mathbf{x})$
Grid purchase cost	15.0	13.6	63.1	52.5
Grid delivery revenue	0.0	0.0	0.1	0.0
Fuels cost	376.4	379.6	214.6	218.6
EV charging cost	7.4	2.8	18.0	5.7
EV discharging revenue	14.1	0.0	37.8	0.0
Grid emission cost	0.3	0.2	0.9	0.8
Generators emission cost	6.6	6.7	3.7	3.7
Total cost	**391.6**	**402.9**	**262.5**	**281.3**

Computational efforts obtained by running the procedure on a 64-bit workstation equipped with 3.50 GHz processor and 16 MB RAM and exploiting virtual parallel calculus on 4 processors are synthetically compared in Table 6. It can be seen that the problem solution takes from 3 min to 22 min to reach an optimal solution where error levels are below selected thresholds, and this time is well compatible with day-ahead programming horizon. The solution involves heavier computations (either number of iterations or computation time) in the presence of $f_1(\mathbf{x})$ objective, due to the involvement of conflicting terms in the objective function, see positive and negative cost contribution due to EV charge and discharge, respectively, in (10). The determination of initial solution is quite fast and does not affect remarkably the total solution time.

Table 6. Computational effort and solution convergence.

	Residential		Commercial	
	$f_1(\mathbf{x})$	$f_2(\mathbf{x})$	$f_1(\mathbf{x})$	$f_2(\mathbf{x})$
Computation time initial condition [s]	0.048	0.162	0.046	0.161
Computation time solution procedure [s]	685.2	797.3	1323.0	197.1
Iteration n.	19	53	182	45
Relative error on variables	$8.50\cdot10^{-5}$	$8.08\cdot10^{-5}$	$9.05\cdot10^{-5}$	$8.88\cdot10^{-5}$
Relative error on constraints	$7.12\cdot10^{-5}$	$4.82\cdot10^{-5}$	$6.94\cdot10^{-6}$	$6.37\cdot10^{-5}$

4. Conclusions

In this paper, strategies for optimal day-ahead operation planning of MG integrating V2G-based EV fleets have been proposed. The procedure, involving electric and thermal load coverage, has been tested on a selected MG configuration, where typical load profiles of residential and commercial users have been considered. The presence of different goals, according to various interaction frameworks between EV aggregator and MG operator, have yielded different operation plans, with particular regard to EV exploitation. Indeed, the presence of suitable cost schemes for EV charge and discharge, in the presence of EV aggregator relating with MG operator, have led to a deeper EV exploitation and a more efficient operation of MG resources, achieving lower total MG cost. Whereas, wearing cost drives the preservation of EVs lifetime, preventing their depletion and providing a service only by defining optimal charging intervals. V2G behavior has allowed the coverage of demand peaks, and can be efficiently utilized when high electricity price occurs. Moreover, the presence of CHPs and ESS has brought to reduce the need of electricity purchase from the external grid to charge EVs. The proposed methodology has proved powerful to deal with the operation planning problem in a suitable time for day-ahead horizon. In addition, the method can be further extended to take into account several EV fleets, characterized by different exigencies, and can be exploited to enhance the integration of V2G in different locations. The implementation and test of obtained results in the envisaged extended configuration of the MG testbed facility is planned to be object of future developments, as well as the setup of the short-term operation management procedure to deal with real time variations to the plan.

Appendix

SQP algorithm solves a sequence of optimization sub-problems, characterized by a quadratic model of the main problem. The basis of the algorithm consists of the calculation of Lagrangian function $L(\mathbf{x})$ related to problem (9), defined as follows:

$$L(\mathbf{x}) = f(\mathbf{x}) + \sum_{w} \lambda_w \cdot g_w(\mathbf{x}) + \sum_{b} \mu_b \cdot h_b(\mathbf{x}) \tag{A.1}$$

where w is the generic equality constraint and λ_w is the correspondent Lagrangian multiplier, whereas b is the generic inequality constraint and μ_b is the correspondent Lagrangian multiplier. It is assumed that bound constraints are expressed as inequality constraints. Therefore, Karush-Kuhn-Tucker (KKT) conditions are posed and approximated by means of second-term truncated Taylor series, thus obtaining, for the κ-th iteration, the following quadratic subproblem:

$$\begin{aligned} &\min_{\mathbf{d}} \nabla f\left(\mathbf{x}^{\kappa}\right)^{T} \cdot \mathbf{d}^{\kappa} + \frac{1}{2}\mathbf{d}^{\kappa} \cdot \mathbf{H}^{\kappa} \cdot \mathbf{d}^{\kappa} \\ &\text{s.t.} \begin{cases} \nabla g_w\left(\mathbf{x}^{\kappa}\right)^{T} \cdot \mathbf{d}^{\kappa} + g_w\left(\mathbf{x}^{\kappa}\right) = 0 \\ \nabla h_b\left(\mathbf{x}^{\kappa}\right)^{T} \cdot \mathbf{d}^{\kappa} + h_b\left(\mathbf{x}^{\kappa}\right) \leq 0 \end{cases} \end{aligned} \tag{A.2}$$

where $\mathbf{H}^{\kappa} = \nabla_{\mathbf{x}}^{2} L\left(\mathbf{x}^{\kappa}, \boldsymbol{\lambda}^{\kappa}, \boldsymbol{\mu}^{\kappa}\right)$ is the Hessian matrix of KKT conditions at the κ-th iteration and $\mathbf{d}^{\kappa}$ is the solution search direction. For each iteration, the algorithm updates the Hessian matrix through an approximate gradient evaluation method, therefore solves the quadratic subproblem (A.2), that can be modified in order to account for feasibility limits (for instance by means of a quadratic approximation of constraints instead of linear) and updates the solution as follows:

$$\mathbf{x}^{\kappa+1} = \mathbf{x}^{\kappa} + \alpha^{\kappa} \cdot \mathbf{d}^{\kappa} \tag{A.3}$$

where α^{κ} is the step-length parameter, determined in order to decrease a merit function, with larger penalty contribution of active constraints.

References

[1] J. Wang, A. Conejo, C. Wang, J. Yan, “Smart grids, renewable energy integration, and climate change mitigation- Future electric energy systems”, Applied Energy, vol. 96, August 2012, pp. 1-3.

[2] A. Gaviano, K. Weber, C. Dirmeier, “Challenges and integration of PV and wind energy facilities from a smart grid point of view,” Energy Procedia, vol. 25, pp. 118–125, 2012.

[3] J. M. Guerrero, M. Chandokar, T. Lee, P. C. Loh, “Advanced control architectures for intelligent microgrids—Part I: Decentralized and hierarchical control,” IEEE Trans. Ind. Electron., vol. 60, no. 4, pp. 1254–1262, Apr. 2013.

[4] Y. Wang, O. Sheikh, B. Hu, C.-C. Chu, R. Gadh, “Integration of V2H/V2G hybrid system for demand response in distribution network”, in:2014 IEEE Int. Conf. on Smart Grid Communications, Nov. 2014, pp. 812–817.

[5] Y. Ota, H. Taniguchi, T. Nakajima, K.M. Liyanage, J. Baba, A. Yokoyama, “Autonomous distributed V2G (Vehicle-to-Grid) satisfying scheduled charging”, IEEE Trans. Smart Grid 3 (March (1)) (2012) 559–564.

[6] E. Sortomme and M. A. El-Sharkawi, “Optimal charging strategies for unidirectional vehicle-to-grid,” IEEE Trans. Smart Grid, vol. 2, no. 1, pp. 131–138, Mar. 2011.

[7] C. Sabillon Antunez, J.F. Franco, M.J. Rider, R. Romero "A New Methodology for the Optimal Charging Coordination of Electric Vehicles Considering Vehicle-to-Grid Technology." IEEE Trans. Sust. Energy, vol. 7, no. 2, pp. 596-607, Apr. 2016.

[8] A. Kavousi-Fard, T. Niknam, M. Fotuhi-Firuzabad, "Stochastic reconfiguration and optimal coordination of V2G plug-in electric vehicles considering correlated wind power generation", IEEE Trans. Sust. Energy, vol. 6, no. 3, pp. 822–830, Jul. 2015.

[9] M. González Vayá, G. Andersson, "Self Scheduling of Plug-In Electric Vehicle Aggregator to Provide Balancing Services for Wind Power," IEEE Trans. Sust. Energy, vol. 7, no. 2, pp. 886-899, Apr. 2016.

[10] Y. Wang, H. Nazaripouya, C.-C. Chu, R. Gadh, H.R. Pota, "Vehicle-to-grid automatic load sharing with driver preference in micro-grids", Proc. of 2014 IEEE PES ISGT Conf. Europe, Oct, 2014, pp. 1–6.

[11] L. Igualada, C. Corchero, M. Cruz-Zambrano, F.-J. Heredia, "Optimal Energy Management for a Residential Microgrid Including a Vehicle-to-Grid System," IEEE Trans. on Smart Grid, vol. 5, no. 4, pp. 2163–2172, Jul. 2014.

[12] V.N. Coelho, I. M. Coelho, B.N. Coelho, M. Weiss Cohen, A.J.R. Reis, S.M. Silva, M.J.F. Souza, P.J. Fleming, F.G. Guimarães, "Multi-objective energy storage power dispatching using plug-in vehicles in a smart-microgrid", Renewable Energy, vol. 89, April 2016, pp. 730–742.

[13] K. M. Tan, V. K. Ramachandaramurthy, J. Y. Yong, "Integration of electric vehicles in smart grid: a review on vehicle to grid technologies and optimization techniques" Renew. Sustain. Energy Rev. 2016, 53, pp. 720-732.

[14] W. Kempton, J. Tomic, "Using fleets of electric-vehicle for grid support". J Power Sources 2007; 168: pp. 459-468.

[15] A. Bracale, G. Carpinelli, F. Mottola, D. Proto, "Single-objective optimal scheduling of a low voltage microgrid: a minimum-cost strategy with peak shaving issues". In: 2012 11th Int. Conf. EEEIC, Venice; May 2012.

[16] A. Brooks, A. Lu, D. Reicher, J. Spirakis, B. Weihl, "Demand dispatch". IEEE Power Energy Mag 2010; vol. 8, pp. 20-29.

[17] Z. Liu, D. Wang, H. Jia, N. Djilali, W. Zhang, "Aggregation and Bidirectional Charging Power Control of Plug-in Hybrid Electric Vehicles: Generation System Adequacy Analysis", IEEE Trans. Sust. Energy, vol. 6 no. 4, pp. 325-335, 2015.

[18] T.N. Le, S. Al-Rubaye, Hao Liang, B.J. Choi, "Dynamic charging and discharging for electric vehicles in microgrids", in Proc. 2015 ICCW London; June 2015 p. 2018-2022.

[19] M. Mao, P. Jin, N. D. Hatziargyriou, L. Chang, "Multiagent-Based Hybrid Energy Management System for Microgrids", IEEE Transactions on Sustainable Energy, vol. 5, no. 3, pp. 938-946, July 2014.

[20] C. Deckmyn, J. Van de Vyver, T. L. Vandoorn, B. Meersman, J. Desmet, L. Vandevelde, "Day-ahead unit commitment model for microgrids", IET Generation, Transmission and Distribution, vol. 11, iss. 1, pp. 1-9, 2017.

[21] H. Kamankesh, V. G. Agelidis, A. Kavousi-Fard, "Optimal scheduling of renewable microgrid considering plug-in hybrid electric vehicle charging demand", Energy, vol. 100, pp. 285-297, 2016.

[22] H. Yang, H. Pan, F. Luo, J. Qiu, Y. Deng, M. Lai, Z. Y. Dong, "Operational Planning of Electric Vehicles for Balancing Wind Power and Load Fluctuations in a Microgrid", IEEE Transactions on Sustainable Energy, Vol. 8, no. 2, April 2017, pp. 592-604

[23] A. G. Anastasiadis, S. Kostantinopoulos, G. P. Kondylis, G. A. Vokas, "Electric vehicle charging in stochastic smart microgrid operation with fuel cell and RES units", International Journal of Hydrogen Energy (2017) http://dx.doi.org/j.ijhydene.2017.01.208

[24] P. Kou, D. Liang, L. Gao, F. Gao, "Stochastic Coordination of Plug-In Electric Vehicles and Wind Turbines in Microgrid: A Model Predictive Control Approach", IEEE Transactions on Smart Grid, vol. 7, no. 3, May 2016, pp. 1537-1551.

[25] A. Ravichandran, S. Sirouspour, P. Malysz, A. Emadi, "A Chance-Constraints-Based Control Strategy for Microgrids with Energy Storage and Integrated Electric Vehicles", IEEE Transactions on Smart Grid, DOI 10.1109/TSG.2016.2552173.

[26] S. M. Moghaddas Tafreshi, H. Ranjbarzadeh, M. Jafari, H. Khayyam, "A probabilistic unit commitment model for optimal operation of plug-in electric vehicles in microgrid", Renewable and Sustainable Energy Reviews, vol. 66, pp. 934-947, 2016.

[27] E. Mortaz, J. Valenzuela, "Microgrid energy scheduling using storage from electric vehicles", Electric Power Systems Research, vol. 143, pp. 554-562, 2017.

[28] S. Mohammadi, S., Soleymani, B. Mozafari, "Scenario-based stochastic operation management of MicroGrid including Wind, Photovoltaic, Micro-Turbine, Fuel Cell and Energy Storage Devices", International Journal on Electric Power and Energy Systems, vol. 54, pp. 525-535, 2014.

[29] D. Wu, D.C. Alyprantis, L. Ying, "Load Scheduling and Dispatch for Aggregators of Plug-In Electric Vehicles", IEEE Trans. Smart Grid, vol. 3, no. 1, March 2012, pp. 368-376.

[30] R.J. Bessa, M.A. Matos, "Forecasting issues for Managing a Portfolio of Electric Vehicles under a Smart Grid Paradigm, Proc. of 2012 IEEE ISGT Europe Conf., Berlin (Germany), pp. 1-8.

[31] Q. Jiang, M. Xue, G. Geng, "Energy management of Microgrid in Grid-Connected and Stand-Alone Modes", IEEE Trans. On Power Systems, vol. 28, no. 3, August 2013, pp. 3380-3389.

[32] M. He, M. Giesselmann, "Reliability-constrained Self-organization and Energy Management towards a Resilient Microgrid Cluster", Proc. of IEEE PES ISGT 2015 Conf., 2015, pp. 1-5.

[33] C. Li, E. Schaltz, J. C. Vasquez, J. M. Guerrero, "Distributed Coordination of Electric Vehicle Charging in a Community Microgrid Considering Real-Time Price", Proc. of IEEE EPE'16 ECCE Europe Conf., pp. 1-8.

[34] L. K. Panwar, S. R. Konda, A. Verma, B. K. Panigrahi, R. Kumar, "Operation window constrained strategic energy management of microgrid with electric vehicle and distributed resources", IET Generation, Transmission and Distribution, vol. 11, iss. 3, pp. 615-626, 2017.

[35] S. Parhizi, A. Khodaei, M. Shahidehpour, "Market-based vs. Price-based Microgrid Optimal Scheduling", IEEE Transactions on Smart Grid, DOI: 10.1109/TSG.2016.2558517

[36] J. E. Contreras-Ocaña, M. R. Sarker, M. A. Ortega-Vazquez, "Decentralized Coordination of a Building Manager and an Electric Vehicle Aggregator", IEEE Transactions on Smart Grid, DOI: 10.1109/TSG.2016.2614768

[37] T. Sherkari, S. Golshannavaz, F. Aminifar, "Techno-Economic Collabroation of PEV Fleets in Energy Management of Microgrids", IEEE Transactions on Power Systems, DOI: 10.1109/TPWRS.2016.2644201

[38] H.S.V.S. Kuman Nunna, S. Battula, S. Doolla, D. Srinivasan, “Energy Management in Smart Distribution Systems with Vehicle-to-Grid Integrated Microgrids”, IEEE Transactions on Smart Grid, DOI: 10.1109/TSG.2016.2646779

[39] V. Hosseinnezhad, M. Rafiee, M. Ahmadian, P. Siano, “Optimal day-ahead operational planning of microgrids”, Energy Conversion and Management, vol. 126, pp. 142-157, 2016

[40] J. Jung, R. P. Broadwater, “Current status and future advances for wind speed and power forecasting”, Renewable and Sustainable Energy Reviews, vol. 31, pp. 762-777, March 2014.

[41] W. Cabrera, D. Benhaddou, C. Ordonez, “Solar Power Preduition for Smart Community Microgrid”, Proc. of 2016 IEEE SMARTCOMP Conf., 18-20 May 2016, St. Louis, MO, U.S.A., pp. 1-6.

[42] A. Dolara, S. Leva, M. Mussetta, E. Ogliari, “PV hourly day-ahead power forecast in a micro grid context”, Proc. of 2016 IEEE EEEIC Conf., Florence, Italy, pp. 1-6

[43] M.J. Sanjari, H. Karami, H.B. Gooi, “Micro-generation dispatch in a smart residential multi-carrier energy system considering demand forecast error”, Energy Conversion and Management, vol. 120, pp. 90-99, 2016.

[44] M. Ross, C. Abbey, F. Bouffard, G. Joos, “Multiobjective optimization dispatch for microgrids with a high penetration of renewable generation”, IEEE Trans. on Sust. Energy, vol. 6 no. 4, pp. 1306-1314, 2015.

[45] B. Zhao, X. Zhang, J. Chen, C. Wang, L. Guo, “Operation optimization of standalone Microgrids considering lifetime characteristics of battery energy storage system,” IEEE Trans. Sust. Energy, vol. 4, no. 4, pp. 934–943, Oct. 2013.

[46] H. Kanchev, F. Colas, V. Lazarov, B. Francois, “Emission reduction and economical optimization of an urban microgrid operation including dispatched PV-based active generators”, IEEE Trans. Sust. Energy, vol. 5, no. 4, pp. 1397-1405, Oct. 2014.

[47] A. Chaouachi, R. M. Kamel, R. Andoulsi, K. Nagasaka, “Multiobjective Intelligent Energy Management for a Microgrid”, IEEE Trans. Ind. Electr., Vol. 60, n. 4, April 2013, pp. 1688-1699.

[48] Z. Wang, L. Wang, A. I. Dounis, R. Yang, “Integration of plug-in hybrid electric vehicles into energy and comfort management for smart building”, Energy Build. 47 (April) (2012) 260–266.

[49] S. Beer, T. Gomez, D. Dallinger, I. Momber, C. Marnay, M. Stadler, and J. Lai, "An economic analysis of used electric vehicle batteries integrated into commercial building microgrids," IEEE Trans. Smart Grid, vol. 3, no. 1, pp. 517–525, 2012.

[50] A.A. Khan, M. Naeem, M. Iqbal, S. Qaisar, A. Anpalagan, "A compendium of optimization objectives, constraints, tools and algorithms for energy management in microgrids", Renew. Sustain. Energy Rev. 2016, 58, pp. 1664-1683.

[51] C.L. Moreira, J.A. Peças Lopes, "MicroGrids Operation and Control under Emergency Conditions", in: A. Keyhani, M. Marwali, "Smart Power Grids 2011", Springer, 2012, pp. 351-399.

[52] M. Falahi, S. Lotfifard, M. Ehsani, K. Butler-Perry, "Dynamic Model Predictive-Based Energy Management of DG Integrated Distribution Systems", IEEE Trans. Power Delivery, vol. 28, no. 4, October 2013, pp. 2217-2227.

[53] M. Restepo, C. A. Canizares, M. Kazerani, "Three-Stage Distribution Feeder Control Considering Four-Quadrant EV Chargers", IEEE Transactions on Smart Grid, Accepted December 2016, http://dx.doi.org/10.1109/TSG.2016.2640202

[54] D. Zhang, S. Evangelisti, P. Lettieri, L.G. Papageorgiou, "Economic and environmental scheduling of smart homes with microgrid: DER operation and electrical tasks", Energy Conversion and Management, vol. 110, pp. 113-124, 2016

[55] Z. Bao, Q. Zhou, Z. Yang, Q. Yang, L. Xu, T. Wu, "A Multi Time-Scale and Multi Energy-Type Coordinated Microgrid Scheduling Solution—Part I: Model and Methodology", IEEE Transactions on Power Systems, vol. 30, No. 5, pp. 2257-2266, Sept. 2015

[56] I. Gerami Moghaddam, M. Saniei, E. Mashhour, "A comprehensive model for self-scheduling an energy hub to supply cooling, heating and electrical demands of a building", Energy, vol. 94, pp. 157-170, 2016.

[57] M. Reyasudin Basir Khan, R. Jidin, J. Pasupuleti, "Multi-agent based distributed control architecture for microgrid energy management and optimization", Energy Conversion and Management, vol. 112, March 2016, pp. 288-307.

[58] J. Fedjaev, S. A. Amamra, B. Francois, "Linear Programming based optimization tool for day ahead energy management of a lithium-ion battery for an industrial microgrid", Proc. of 2016 IEEE PEMC Conf. Varna, Bulgaria, 25-28 Sept. 2016, pp. 406-411.

[59] M. S. Mahmoud, F. M. Al-Sunni, "Control and Optimization of Distributed Generation Systems", Springer, 2015.

[60] A. C. Luna, N. L. Diaz, L. Mengg. M. Graells, J. C. Vasquez, J. M. Guerrero, "Generation-Side Power Scheduling in a Grid-Connected DC Microgrid", Proc. of IEEE IDCM'15 conf., pp. 1-6.

[61] A. Seaman, T.S. Dao, J. McPhee, "A survey of mathematics-based equivalent-circuit and electrochemical battery models for hybrid and electric vehicle simulation", J. Power Sources, vol. 256, pp. 410-423, 2014

[62] NREL (2016), Energy Technology Cost and Performance Data of Distributed Generation: Distributed Generation Energy Technology Operations and Maintenance Costs. Available online: http://www.nrel.gov/analysis/tech_cost_om_dg.html

[63] B. Zhao, X. Zhang, J. Chan, C. Wang, L. Guo, "Operation Optimization of Standalone Microgrids Considering Lifetime Characteristics of Battery Energy Storage System", IEEE Trans. Sust. Energy, vol. 4, no., 4, pp. 934-943, October 2013

[64] W. Su, J. Wang, J. Roh, "Stochatic Energy Scheduling in Microgrids With Intermittent Renewable Energy Resources", IEEE Transactions on Smart Grid, vol. 5, no, 4, pp. 1876-1883, July 2014

[65] C. Zhou , K. Qian , M. Allan, W. Zhou, "Modeling of the cost of EV battery wear due to V2G application in power systems", IEEE Trans. Energy Conversion, vol. 26, no. 4, pp. 1041-1050, 2011.

[66] B. Aluisio, A. Cagnano, E. De Tuglie, M. Dicorato, G. Forte, M. Trovato, "PrInCE lab microgrid: Early experimental results", 2016 AEIT International Annual Conference (AEIT), Capri (Italy), 5-7 Oct. 2016, pp. 1-6

[67] C. T. Nguyen, L. B. Le, "Optimal Bidding Strategy for Microgrids Considering Renewable Energy and Building Thermal Dynamics", IEEE Transactions on Smart Grid, Vol. 4, no. 4, pp. 1608-1620, July 2014

[68] ISPRA, (2015), "Fattori di emissione per la produzione ed il consumo di energia elettrica in Italia", (in Italian). [Online]. Available: http://www.sinanet.isprambiente.it

[69] Idaho National Laboratory, “Nissan Leaf - VIN 0356, Advanced Vehicle Testing - Baseline Testing Results,” Available online: http://avt.inel.gov/pdf/fsev/fact2011nissanleaf.pdf

[70] EERE, “Commercial and Residential Hourly Load Profiles for all TMY3 locations in the United States” [Online]. Available: http://en.openei.org/datasets/dataset

[71] J. Neubauer, E. Wood, “The impact of range anxiety and home, workplace, and public charging infrastructure on simulated battery electric vehicle lifetime utility”, J. Pow. Sources, vol. 257, pp. 12-20, 2014.

[72] A. Hoke, A. Brissette, K. Smith, A. Pratt, D. Maksimovic, “Accounting for Lithium-Ion Battery Degradation in Electric Vehicle Charging Optimization”, IEEE Journal of Emerging and Selectred Topris in Power Electronics”, vol. 2, no. 3, pp. 691-700, September 2014.

[73] T. Gnann, P. Plötz, A. Kühn, M. Wietschel, “Modelling market diffusion of electric vehicles with real world driving data – German market and policy options”, Transportation Research Part A, vol. 77, pp. 95-112, 2015.

[74] Deliberazione AEEG 493/2012 “Approvazione delle modalità per l’attribuzione dei corrispettivi di sbilanciamento e dei corrispettivi a copertura dei costi amministrativi da attribuire ai produttori in regime di ritiro dedicato e di tariffa fissa onnicomprensiva”, Nov. 2012 (in Italian).

[75] http://www.amgasbarisrl.it/

[76] http://www.sendeco2.com

[77] A. Schuller, B. Dietz, C. M. Flath, C. Weinhardt, “Charging strategies for battery electric vehicles: Economic benchmark and V2G potential”, IEEE Trans. Power Syst., vol. 29, no. 5, pp. 2014-2022, 2014.

[78] J. Nocedal, S. J. Wright, “Numerical Optimization, Second Edition”. Springer Series in Operations Research, Springer Verlag, 2006.

[79] F. A. Bayer, G. Notarstefano, F. Allgower, “A Projected SQP method for Nonlinear Optimal Control with Quadratic Convergence”, Proc. of 25nd IEEE Conference on Decision and Control, December 10-13, 2013, Florence, Italy, pp.6463-6468,

[80] P. E. Gill., E. Wong, “Sequential quadratic programming methods”, in: J: Lee, S. Leyffer, “Mixed Integer Nonlinear Programming”, Vol. 147 of The IMA Volumes in Mathematics its Applications, Springer Science, pp. 147-224, 2012.

Published source: http://dx.doi.org/10.1016/j.epsr.2017.07.015

[81] M. A. Gonzalez Chapa, J. R. Vega Galaz, “An Economic Dispatch Algorithm For Cogeneration Systems”, Proc. of 2004 IEEE PES General Meeting, 6-10 June 2004, pp. 1-5.